

INVERSE KINEMATICS AND SINGULARITIES OF MANIPULATORS WITH OFFSET WRIST

Robert L. Williams II

Department of Mechanical Engineering
Ohio University
Athens, OH 45701

IASTED International Journal of Robotics and Automation

Vol. 14, No. 1, pp. 1-8
1999

Contact information:

Robert L. Williams II

Member, IASTED

Assistant Professor

Department of Mechanical Engineering

257 Stocker Center

Ohio University

Athens, OH 45701-2979

phone: (740) 593 - 1096

fax: (740) 593 - 0476

email: bobw@bobcat.ent.ohiou.edu

INVERSE KINEMATICS AND SINGULARITIES OF MANIPULATORS WITH OFFSET WRIST

Robert L. Williams II
Assistant Professor
Department of Mechanical Engineering
257 Stocker Center
Ohio University
Athens, Ohio 45701-2979

ABSTRACT

The double universal joint robot wrist can eliminate singularities which limit the performance of existing industrial robot wrists. Unfortunately, this singularity-free wrist has an offset which prevents decoupling of the position and orientation in the manipulator inverse kinematics problem. Closed-form solutions are difficult, if not impossible, to find. This paper solves the inverse position kinematics problem of manipulators with the double universal joint wrist. Common regional manipulator types are used to demonstrate the solutions. A numerical singularity analysis is presented for manipulators with the offset double universal joint wrist. The results point to the existence of coupled position and orientation singularities which are difficult to enumerate. Therefore, this offset singularity-free wrist actually worsens the overall manipulator singularity problem.

KEY WORDS

Offset robot wrist, Double universal joint robot wrist, Inverse kinematics, Manipulator singularities

1 INTRODUCTION

Most existing industrial robot wrists have singularity configurations which restrict manipulator dexterity. The double universal joint (DUJ) wrist has been proposed to eliminate wrist singularities. The kinematic diagram for this wrist is shown in Fig. 1a. Double universal joint wrists have been designed and built by Trevelyan, et al. [1], Milenkovic [2], and Rosheim [3,4]. The ET Wrist [1] was designed for sheep shearing. The Omni-Wrist [4] is currently used for industrial spray painting operations. Forward and inverse position and velocity kinematics equations for the DUJ wrist are presented in [5]. The present paper studies this class of robot wrist mounted on different regional manipulator arms.

Offset wrists complicate manipulator kinematics and may increase singularity problems. More recently, Stanasic, et al., [6,7] have developed a singularity-free wrist and regional arm structure without the detrimental offset.

The DUJ wrist has an offset separating wrist coordinate frames. This prevents decoupling of manipulator position and orientation, which complicates the inverse position solution. The current paper solves the inverse position problem of the three-degree-of-freedom DUJ wrist on three-degree-of-freedom Cartesian, cylindrical, spherical, and articulated regional arms. Two inverse position solution algorithms are developed: 1) Closed-form solutions are found for two simple manipulator geometries. 2) An iterative solution calculates the arm variables and then the wrist variables in closed-form, iterating until convergence is achieved. Similar methods were presented by Milenkovic [8] and Takano [9]. A good initial guess is calculated for the iteration by assuming zero wrist offset and using standard decoupling of position and orientation. In ensuing steps the wrist offset is included, each time using the current wrist angles to calculate the input to the position part. In this way the Cartesian position error is driven towards zero. The orientation error is theoretically zero at each step.

This paper first discusses the inverse position problem and demonstrates why the DUJ wrist complicates the problem. The inverse position solution methods are then developed. Lastly, a singularity analysis is presented for manipulators with the DUJ wrist to investigate coupled position and orientation singularities.

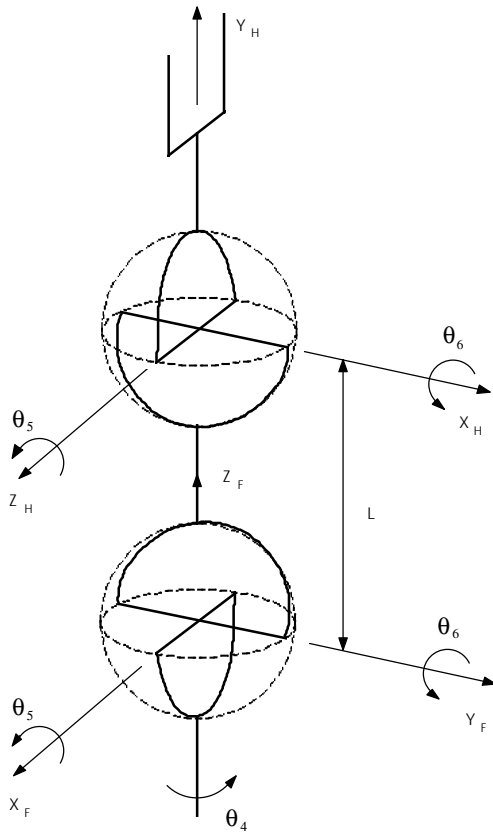


Figure 1a
Double Universal Joint (DUJ) Wrist

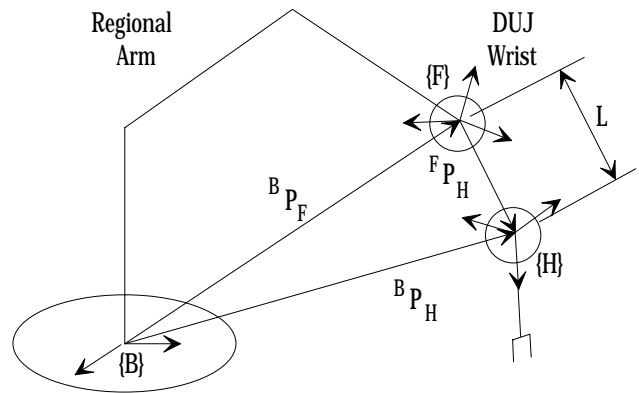


Figure 1b
Manipulator with DUJ Wrist

2 INVERSE POSITION PROBLEM

The forward kinematics problem is a mapping from joint space θ to Cartesian space y . For serial manipulators, the forward kinematics problem is straightforward [10].

$$y = f(\theta) \quad (1)$$

The inverse position kinematics problem inverts Eq. 1, mapping the Cartesian space to joint space. Equation 2 is difficult to solve because the system is coupled, nonlinear, and multiple solutions generally exist.

$$\theta = f^{-1}(y) \quad (2)$$

The forward kinematics solution may be expressed as a concatenation of homogeneous transformation matrices, factored at the forearm frame.

$${}^B_H T = {}^B_F T(\theta_1, \theta_2, \theta_3) {}^F_H T(\theta_4, \theta_5, \theta_6) \quad (3)$$

The inverse position kinematics problem uses the same equations, but ${}^B_H T$ is specified and the joint angles are unknown.

2.1 Manipulator Wrists with Collocated Frames

Most industrial wrists are spherical, with three coincident frames. Pieper [11] proved that if a manipulator has three consecutive joints with collocated frames, a closed-form inverse position solution exists. For a spherical wrist, this solution can be found by decoupling the Cartesian position and orientation. The forearm frame $\{F\}$ origin is always collocated with the last wrist frame $\{H\}$ origin, and so the Cartesian position is only a function of the arm joint values $(\theta_1, \theta_2, \theta_3)$.

$$\{P_X \quad P_Y \quad P_Z\}^T = {}^B P_F(\theta_1, \theta_2, \theta_3) \quad (4)$$

After solving these arm joint values, the relative wrist orientation is found:

$${}^F_H R = {}^B_F R^{-1} {}^B_H R = {}^B_F R^T(\theta_1, \theta_2, \theta_3) {}^B_H R \quad (5)$$

With ${}^F_H R$ known, the wrist angles $(\theta_4, \theta_5, \theta_6)$ are found by inverting the appropriate Euler angle set.

2.2 Double Universal Joint (DUJ) Wrist

For the DUJ wrist (and other non-spherical wrists), the Cartesian position and orientation are coupled because ${}^F P_H$ (the position vector from the forearm to the last wrist frame origin) is nonzero. (See Fig. 1b, where the offset L is exaggerated). The Cartesian position is a function of all joint angles.

$$\{P_X \quad P_Y \quad P_Z\}^T = {}^B P_H(\theta_1, \theta_2, \theta_3, \theta_4, \theta_5, \theta_6) \quad (6)$$

Three more equations are obtained from the orientation command. These six equations are nonlinear and coupled in the six unknowns. A closed-form solution may not exist.

The following equation is an attempt to decouple Eqs. 6 (see Fig. 1b).

$${}^B P_F = {}^B P_H - {}^B R^F P_H \quad (7)$$

This fails because ${}^F P_H$ depends on $(\theta_4, \theta_5, \theta_6)$.

3 INVERSE POSITION SOLUTION

Two methods are used to solve the inverse position kinematics of manipulators with the DUJ wrist. Closed-form solutions were found for two manipulators. An iterative method was applied to manipulators with no closed-form solution.

Figures 2a through 2d show the three-degree-of-freedom regional arms considered in this paper. Each arm has a base frame $\{B\}$ and a forearm frame $\{F\}$ where the DUJ wrist is mounted. The last wrist frame is $\{H\}$ in Fig. 1. The articulated arm (Fig. 2d) is based on the Flight Telerobotic Servicer (FTS) arm [12] with the first joint locked. Though not currently scheduled for space flight, FTS flight hardware has been built for NASA. Originally, the offset DUJ wrist was considered for the FTS hardware. Details for the solutions discussed below are given in [13] and [5].

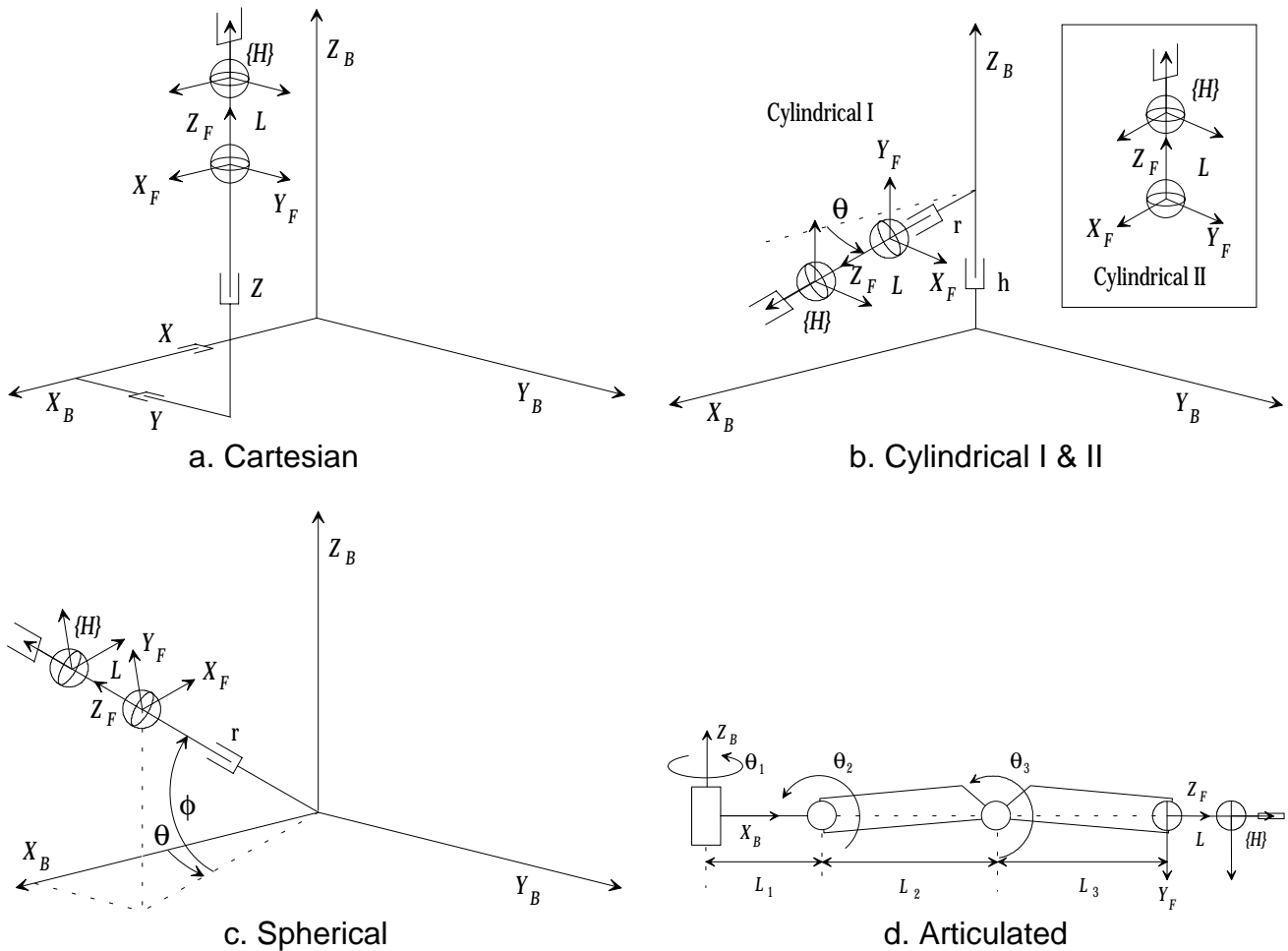


Figure 2
Regional Arms with DUJ Wrist

3.1 Closed-Form Solutions

A closed-form solution was developed for the Cartesian manipulator. The basis for this solution is that the forearm orientation is independent of the arm variables (X,Y,Z) : ${}^B_R = I$, so ${}^F_R = {}^B_R$. The wrist angles are calculated as in the Appendix. Then Eq. 7 is used to calculate the unknowns (X,Y,Z) ; the abbreviations $c_i = \cos \theta_i$ and $s_i = \sin \theta_i$ are used throughout this paper.

$$\begin{Bmatrix} X \\ Y \\ Z \end{Bmatrix} = \begin{Bmatrix} P_X \\ P_Y \\ P_Z \end{Bmatrix} - \begin{Bmatrix} L(c_4s_6 + s_4s_5c_6) \\ L(s_4s_6 - c_4s_5c_6) \\ Lc_5c_6 \end{Bmatrix} \quad (8)$$

A closed-form solution for the cylindrical I manipulator of Fig. 2b was attempted. Though this attempt failed, a closed-form solution was found for the cylindrical II manipulator. The difference between the cylindrical manipulators is the mounting orientation of the DUJ wrist, as seen in Fig. 2b. For either cylindrical manipulator, B_R is a function of unknown θ_2 . Therefore, Eq. 5 may not be applied to solve $(\theta_4, \theta_5, \theta_6)$ first, as in the Cartesian case. Rather, the kinematics equations, Eq. 3, are used to solve for (h, θ, r) first. The key to the cylindrical II solution is the following combination of unknowns; r_{32} is given from the orientation command.

$$c_5c_6 = \sqrt{\frac{r_{32} + 1}{2}} \quad (9)$$

The position and orientation is decoupled using Eq. 9. The solution is:

$$h = P_Z - Lc_5c_6 \quad \theta = \tan^{-1}\left(\frac{B}{A}\right) \quad r = \sqrt{A^2 + B^2} \quad (10)$$

where:

$$A = P_X - \frac{Lr_{12}}{2c_5c_6} \quad B = P_Y - \frac{Lr_{22}}{2c_5c_6}$$

There is a unique solution, assuming $r > 0$ and using the quadrant-specific inverse tangent function. Following this solution, Eq. 5 is used to find F_R , and $(\theta_4, \theta_5, \theta_6)$ are calculated as in the Appendix.

3.2 Iterative Solution Method

The closed-form solutions presented in the previous section are for special cases. For general manipulators with the DUJ wrist, the offset L prevents decoupling of the arm and wrist unknowns. The iterative method for solving the inverse position kinematics of a manipulator with offset wrist axes applies to any arbitrary 3-dof regional arm structures. The efficiency is improved if the 3-dof regional arm has a closed-form inverse kinematics solution. The algorithm flow-chart is shown in Fig. 3. This algorithm is not new as similar methods have been presented [8, 9]. Thus, the efficiency of the iterative method presented is comparable to these earlier works.

To provide a good initial guess, the wrist offset L is first assumed to be zero, so ${}^B P_F = {}^B P_H$. With this condition, the solution method follows Eqs. 4 and 5. The solutions for the first three joints given (P_X, P_Y, P_Z) are given in the Appendix for the cylindrical I, spherical, and articulated arms. After solving the first three joint values, the wrist unknowns $(\theta_4, \theta_5, \theta_6)$ are solved in the Appendix, given ${}^F_H R$ from Eq. 5. In the next iteration, Eq. 7 is used to obtain a better value for ${}^B P_F$ than the zero-offset assumption yields. This equation may be applied because approximate values for the wrist joints have been calculated. The updated ${}^B P_F$ is used to repeat the calculations, solving the arm and then wrist unknowns.

A benefit of this method is that the orientation error is zero at each iteration. The $(\theta_4, \theta_5, \theta_6)$ values are not the exact solution. However, they produce the exact commanded orientation because they are based on ${}^B_F R$ (calculated from the current values for the first three joints) and the original ${}^B_H R$.

The position vector error resulting from each iteration is expressed by the scalar Cartesian position error (CPE). The commanded position vector is ${}^B P_H$; the actual position vector is ${}^B P_{H_E}$, calculated from forward kinematics using the current joint values. CPE is calculated using the Euclidean norm in Eq. 11. The algorithm terminates when CPE is less than a specified tolerance ϵ .

$$CPE = \left\| {}^B P_H - {}^B P_{H_E} \right\| \quad (11)$$

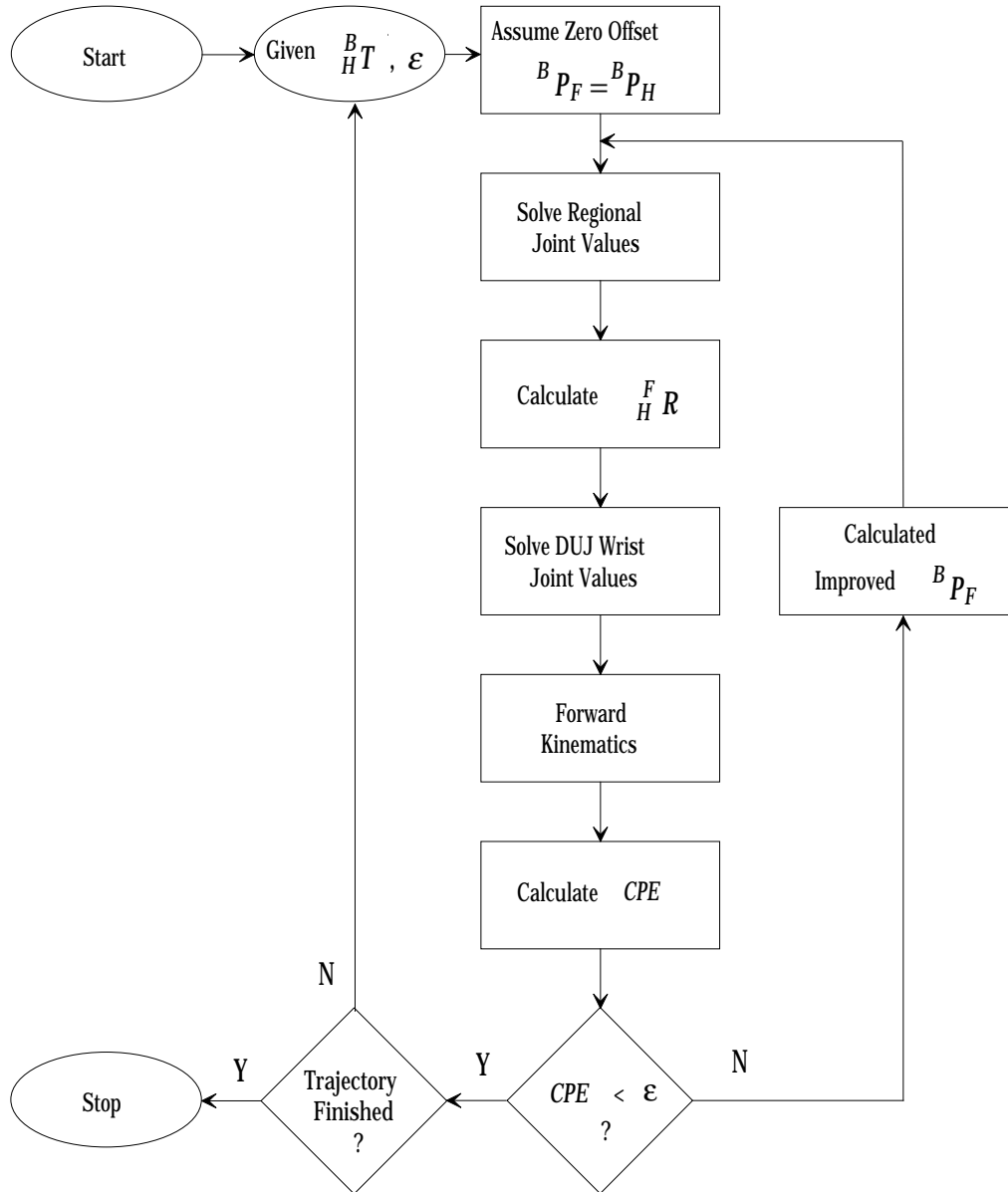


Figure 3
Iterative Inverse Kinematics Algorithm

The number of multiple inverse position solutions is summarized in Table 1, both for the regional arm alone and the overall manipulator including DUJ wrist. Table 1 assumes prismatic joints are limited to positive values. The DUJ wrist alone has four multiple solutions so the total number of solutions is $4x$, where x is the number of regional arm multiple solutions. Four solutions are found for the DUJ wrist even when the offset L is set to zero to calculate the initial guess for iteration. The iterative method finds all possible multiple solutions as summarized in Table 1.

Table 1 Number of Inverse Solutions

Manipulator	Regional Solutions	Overall Solutions
Cartesian	1	4
Cylindrical I & II	1	4
Spherical	2	8
Articulated	4	16

Figure 4 shows the convergence of the iterative method for the cylindrical, spherical, and articulated manipulators given a specific $\frac{B}{H}T$, where N is the number of iterations. After the first iteration, $CPE = L$ (41 mm from a commercial DUJ wrist) for all manipulators. In each iteration, CPE decreases approximately by an order of magnitude. Closed-form solutions are used for each iteration to reduce computation.

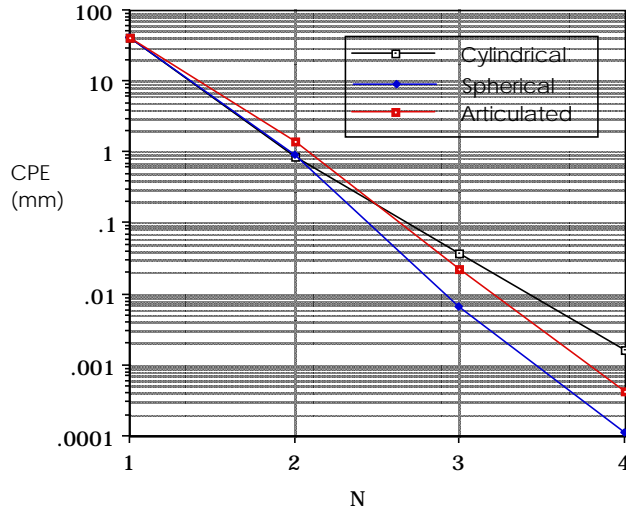


Figure 4 Convergence of Iterative Algorithm

No formal convergence proof is available. The algorithm performed similar to Fig. 4 for all simulated trajectories (Fig. 4 is for one commanded $\frac{B}{H}T$ along a trajectory). As long as the offset L is small relative to the smallest effective moment arm due to the regional arm lengths, convergence is likely. However, for certain configurations (such as when the last wrist frame is placed near the first regional joint) the inverse position solution may diverge. In such cases, the linearized resolved-rate control method [14] may be used in place of inverse position because it is not iterative and can handle the offset. Both inverse position and resolved rate algorithms are subject to the same singularities, presented in the next section.

4 MANIPULATOR SINGULARITY ANALYSIS

Manipulator singularities for non-redundant manipulators are found from the determinant of the manipulator Jacobian matrix J . All joint angle sets which result in zero or near zero determinant are at or near singular configurations. Singularities instantaneously cause the loss of one or more degrees of freedom. In the neighborhood of singularities, a finite Cartesian velocity command requires joint velocities approaching infinity.

For a manipulator with a spherical wrist, the upper right Jacobian submatrix is the zero matrix, which is the velocity-domain manifestation of position/orientation decoupling (see Eq. 12, where $\{v \ \omega\}^T = [J]\{\dot{\Theta}\}$; v are the three translational Cartesian velocities, ω are the three rotational Cartesian velocities, and $\{\dot{\Theta}\}$ are the six joint rates). Singularities are classified as regional arm singularities (found from $|J_{UL}| = 0$) and wrist singularities (found from $|J_{LR}| = 0$).

$$[J] = \begin{bmatrix} [J_{UL}] & [0] \\ [J_{LL}] & [J_{LR}] \end{bmatrix}; \quad |J| = |J_{UL}||J_{LR}| \quad (12)$$

For a manipulator with an offset wrist the Jacobian matrix $[\bar{J}]$ is fully populated as shown in Eq. 13. This is because the wrist joints participate in translation of the last wrist frame in addition to orientation. In this case, the singularities can no longer be classified as separate regional arm singularities and wrist singularities.

$$[\bar{J}] = \begin{bmatrix} [\bar{J}_{UL}] & [\bar{J}_{UR}] \\ [\bar{J}_{LL}] & [\bar{J}_{LR}] \end{bmatrix}; \quad |\bar{J}| \neq |\bar{J}_{UL}||\bar{J}_{LR}| \quad (13)$$

For two manipulators identical except for wrist offset L : $[\bar{J}_{UL}] \neq [J_{UL}]$ due to the additional moment arm L affecting Cartesian translational rates from the regional arm joint rates; $[\bar{J}_{UR}] \neq [J_{UR}] = [0]$ because in the offset wrist case the wrist joint rates enter into the Cartesian translational rates; however, $[\bar{J}_{LL}] = [J_{LL}]$ and $[\bar{J}_{LR}] = [J_{LR}]$ because the wrist offset has no effect on the Cartesian rotational rates.

The DUJ wrist alone is singularity-free (actually, the two existing singularities are forced to lie outside of joint limits, as shown in [4, 5]). The regional arm singularities for the first three joints do not necessarily exist for the overall manipulator with offset wrist. The following question arises: Are there any singularities due to the coupling of position and orientation? This question is answered by analyzing the determinant of the 6x6 Jacobian matrix for each manipulator with the DUJ wrist. This analysis has not been previously published, to the author's knowledge.

The overall Jacobian matrix for a manipulator with the DUJ wrist (Eq. 13) can be determined symbolically or numerically given the DH parameters (see tables in the Appendix). The method used in this paper recognizes each column i of the Jacobian matrix as the contribution to the Cartesian velocity of the last wrist frame $\{v \ \omega\}^T$ due to joint i alone, with $\dot{\theta}_i$ factored out for revolute joints (or \dot{d}_i for prismatic joints). Equation 14 gives the 6x1 i^{th} column of the Jacobian matrix when the i^{th} joint is revolute (left) and prismatic (right).

$${}^k\{J\}_i = \begin{cases} {}^k\hat{Z}_i \times {}^k({}^iP_H) \\ {}^k\hat{Z}_i \end{cases} \quad {}^k\{J\}_i = \begin{cases} {}^k\hat{Z}_i \\ 0 \end{cases} \quad (14)$$

where ${}^k\{J\}_i$ is the i^{th} column of the Jacobian matrix expressed in $\{k\}$ coordinates, ${}^k\hat{Z}_i$ is the instantaneous direction of the revolute axis (or sliding direction for prismatic joints), and ${}^k({}^iP_H)$ is the position vector from the origin of frame i to the origin of the last wrist frame H , expressed in $\{k\}$ coordinates. Equation 14 holds for manipulators without and with wrist offset (Eq. 12 and Eq. 13, respectively).

All manipulators considered in this paper have a 3-dof regional arm with the 3-dof DUJ wrist. However, the Jacobian matrix for all cases (given the DH parameters in the Appendix) will be derived as a 6x8 matrix due to the repeated angles θ_5, θ_6 in Fig. 1a. Since the DUJ wrist is designed so both angles θ_5 and angles θ_6 are individually coupled, columns 5 and 8 of this 6x8 Jacobian both multiply $\dot{\theta}_5$ and columns 6 and 7 multiply $\dot{\theta}_6$. Therefore, the original 6x8 Jacobian matrix is converted to a 6x6 Jacobian matrix by adding columns 5 and 8 to form column 5, and adding columns 6 and 7 to form column 6.

A potential problem in rate kinematics and singularity analysis is Jacobian matrix scaling. If the translational and rotational terms have significantly different scales, the resulting Jacobian matrix conditioning will be in question. For instance, in this paper the DH length parameters were chosen on the order of 1 *m*. The Jacobian matrix scaling will be acceptable since all rotational terms are constrained to be unit vectors or zero (see Eq. 14) and the translational terms will be the same order of magnitude. If however 1000 *mm* were used instead of 1 *m*, the Jacobian matrix scaling would suffer.

For Jacobian matrices derived symbolically, the simplest terms will result if the frame of expression is in the middle of the serial chain, usually the elbow frame. Note that regardless of the frame *k* of expression, the Jacobian matrix always relates the last wrist frame Cartesian rates with respect to the base frame. The Jacobian determinant is invariant with regard to coordinate transformations. Singularity conditions are reported below for the manipulators in this paper.

4.1 Symbolic Singularity Analysis

The Jacobian matrix determinant for the Cartesian manipulator with the DUJ wrist is Eq. 15.

$$|\bar{J}| = 4c_5c_6^2 = 0 \quad (15)$$

Due to the simple geometry of the Cartesian manipulator, Eq. 15 is identical to the determinant of the 3x3 Jacobian matrix for the wrist alone [5]. The singularity conditions are solved by inspection, $\theta_5 = \pm 90^\circ$ or $\theta_6 = \pm 90^\circ$. If the wrist is designed such that these angles are beyond joint limits, the Cartesian manipulator with the DUJ wrist is singularity-free.

As manipulator complexity increases, the symbolic complexity of the Jacobian matrix determinant also increases. The remaining singularity conditions are derived via exhaustive computer numerical searches. Partial symbolic results are possible for the cylindrical I, cylindrical II, and spherical manipulators: These determinants each have a factor c_6 , so $\theta_6 = \pm 90^\circ$ is a singularity condition for these manipulators; as mentioned above, this lies beyond joint limits.

4.2 Numerical Singularity Analysis

Both cylindrical I and cylindrical II manipulators with the DUJ wrist were found to be singularity-free. The angle θ was varied over 360° in one degree steps, while θ_5 and θ_6 were varied over $\pm 50^\circ$ (the commercial wrist in [4] has $\pm 45^\circ$ limits). No determinant was less than 0.2 for either case. The cylindrical manipulators both have singular conditions $r=0$, and $\theta_6 = \pm 90^\circ$ but these are assumed to be outside joint limits. Several coupled position and orientation singularities were found when θ_5 and θ_6 were extended beyond $\pm 50^\circ$, but these cases are outside wrist joint limits.

Three standard singularity conditions were identified for the spherical manipulator with DUJ wrist: 1) $\theta_6 = \pm 90^\circ$; 2) $r=0$ and $\phi = 0$; and 3) $r=0$ and $\theta_6 = 0$. None of these standard singular conditions cause a problem because $\theta_6 = \pm 90^\circ$ and $r=0$ are outside joint limits. However, in addition the spherical manipulator has many coupled position and orientation singularities internal to its workspace, found by numerical searching. It is difficult to assign a numerical value delineating singularity, but generally any determinant less than 10^{-6} is in the neighborhood of a singularity, given acceptable Jacobian matrix scaling. The singular conditions occur at general angular values within the DUJ wrist and regional arm joint limits.

The behavior of the articulated manipulator with the DUJ wrist is similar to that of the spherical manipulator. There are many coupled position and orientation singularities existing at various locations within the workspace, determined by exhaustive numerical searching. Locations for these singularities are difficult to enumerate. Again, the singular conditions occur at general angular values within practical joint limits.

In summary, for simple manipulator geometries (the Cartesian manipulator and both cylindrical manipulators), the DUJ wrist does not cause coupled singularities. These manipulators are singularity-free (except for workspace limit singularities, which no manipulator can escape). As the manipulator geometry becomes more complex, many coupled position and orientation singularities arise within the workspace, at general configurations difficult to enumerate. The author is currently applying screw theory in attempt to explain these singularities geometrically, which are less easy to understand than singularities of common industrial manipulators with zero-offset wrists.

5 CONCLUSION

This paper presents solution of the inverse position problem and singularity analysis for the offset DUJ wrist on a manipulator. The offset of this singularity-free wrist prevents decoupling of the position and orientation. Cartesian, cylindrical, spherical, and articulated regional manipulators were considered. Closed-form solutions are found for the Cartesian and cylindrical II manipulators. The iterative method is numerical, but each iteration uses closed-form solutions. It was found that two iterations give 1 *mm* accuracy for all three cases considered. A good initial guess is calculated, all possible multiple solutions are found, and the method is based on closed-form solutions.

A manipulator singularity analysis using the Jacobian matrices of the Cartesian, cylindrical I and II, spherical, and articulated arms with the DUJ wrist was presented. It was found that the Cartesian and cylindrical I and II manipulators are singularity-free when using the wrist. Coupled position and orientation singularities were found at many locations within the spherical and articulated manipulators' workspaces and within DUJ wrist joint limits. This is a potentially serious limitation of the wrist, when used on common regional manipulator types.

The methods of this paper can be implemented in a real-time controller for manipulators with the DUJ wrist. Such dexterous manipulators could be used in space telerobotic systems and industrial and remote applications, but further work is required to avoid the singularities. The primary contribution of this paper is exposing the existence of coupled position and orientation singularities in manipulators with the offset DUJ wrist. These singularities were found to occur at general configurations difficult to enumerate. Thus, the irony is that offset singularity-free wrists may actually exacerbate the manipulator singularity problem.

6 REFERENCES

- [1] Trevelyan, J.P., Kovese, P.D., Ong, M., and Elford, D., 1986, "ET: A Wrist Mechanism Without Singular Positions", *The International Journal of Robotics Research*, Vol. 4, No. 4, pp. 71-85.
- [2] Milenkovic, V., 1987, "New Nonsingular Robot Wrist Design", *Robots 11 Conference Proceedings RI/SME*, Chicago, IL, pp. 13.29-13.42.
- [3] Rosheim, M.E., 1989, **Robot Wrist Actuators**, John Wiley & Sons, New York.
- [4] Rosheim, M.E., 1987, "Singularity-Free Hollow Spray Painting Wrists", *Robots 11 Conference Proceedings RI/SME*, Chicago, IL, pp. 13.7-13.28.
- [5] Williams, R.L., II, 1990, "Forward and Inverse Kinematics of Double Universal Joint Robot Wrists", *Proceedings of the 1990 Space Operations, Applications, and Research (SOAR) Symposium*, Albuquerque, NM.
- [6] Stanasic, M.M., and Remis, S.J., 1994, "Design of a Singularity-Free Articulated Arm-Subassembly", *IEEE Transactions on Robotics and Automation*.
- [7] Stanasic, M.M., and Duta, O., 1990, "Symmetrically Actuated Double Pointing Systems: The Basis of Singularity-Free Robot Wrists", *IEEE Transactions on Robotics and Automation*, Vol. 6, No. 5.
- [8] Milenkovic, V., and Huang, B., 1983, "Kinematics of Major Robot Linkage", *Robots 7 Conference Proceedings RI/SME*, Chicago, IL, pp. 16.31 - 16.42.
- [9] Takano, M., 1985, "A New Effective Solution to Inverse Kinematic Problem (Synthesis) of a Robot With Any Type of Configuration", *Journal of the Faculty of Engineering, The University of Tokyo*, Vol. 38, No. 2, pp. 107-135.
- [10] Craig, J.J., 1989, **Introduction to Robotics: Mechanics and Control**, Addison Wesley Publishing Co., Reading, MA.
- [11] Pieper, D., 1968, "The Kinematics of Manipulators Under Computer Control ", *Ph.D. Thesis*, Stanford University.
- [12] Krauze, L.D., Schlagel, J.H., and Henry, P.L., 1990, "Space Station Telerobotic Servicer (FTS) Phase C/D DTF-1 Manipulator/End Effector Kinematic Analysis", *Final Report, Contract NAS5-30689*, Martin Marietta Astronautics Group.
- [13] Williams, R.L., II, 1992, "The Double Universal Joint Wrist on a Manipulator: Solution of Inverse Position Kinematics and Singularity Analysis", *NASA Technical Memorandum 104212*.
- [14] Whitney, D.E., 1969, "Resolved Motion Rate Control of Manipulators and Human Prostheses", *IEEE Trans. on Man-Machine Systems*, Vol. 10, pp. 47-53.

APPENDIX. INVERSE POSITION SOLUTIONS

Inverse position solutions are presented in this appendix for the DUJ wrist, plus the cylindrical I, spherical, and articulated regional arms. For each case, the forward kinematics transformation is given, from which the inverse position solution is derived (except for the Cartesian and Cylindrical II, whose closed-form solutions were presented in Section 3.1. First, the DH parameters (Craig convention, [10]) are given for the DUJ wrist and each regional arm. For more detail, refer to [5, 13].

Double Universal Joint (DUJ) Wrist

Table A.1 DUJ Wrist DH Parameters

i	α_{i-1}	a_{i-1}	d_i	θ_i
4	0	0	0	$\theta_4 + 90^\circ$
5	90°	0	0	$\theta_5 + 90^\circ$
6	90°	0	0	θ_6
7	0	L	0	θ_6
H	-90°	0	0	$\theta_5 - 90^\circ$

$$\begin{bmatrix} F \\ H \\ T \end{bmatrix} = \begin{bmatrix} 2s_5c_6K_1 - s_4 & 2c_5c_6K_1 & -2s_6K_1 + c_4 & LK_1 \\ 2s_5c_6K_2 + c_4 & 2c_5c_6K_2 & -2s_6K_2 + s_4 & LK_2 \\ 2s_5c_5c_6^2 & 2c_5^2c_6^2 - 1 & -2c_5s_6c_6 & Lc_5c_6 \\ 0 & 0 & 0 & 1 \end{bmatrix}$$

where: $K_1 = c_4s_6 + s_4s_5c_6$ $K_2 = s_4s_6 - c_4s_5c_6$

$$\theta_4 = 2 \tan^{-1} \left(\frac{r_{23} - r_{11}}{r_{13} + r_{21} + r_{32} + 1} \right) \quad \theta_5 = \tan^{-1} \left(\frac{r_{13}s_4 - r_{23}c_4}{r_{33}} \right)$$

$$\theta_6 = \frac{1}{2} \tan^{-1} \left(\frac{(r_{23}c_4 - r_{13}s_4)s_5 - r_{33}c_5}{r_{13}c_4 + r_{23}s_4} \right)$$

There are four possible solutions, ignoring joint limits.

Cartesian Regional Arm

Table A.2 Cartesian DH Parameters

i	α_{i-1}	a_{i-1}	d_i	θ_i
1	0	X	0	90°
2	0	Y	0	-90°
3	0	0	Z	0

Cylindrical I Regional Arm

Table A.3 Cylindrical I DH Parameters

i	α_{i-1}	a_{i-1}	d_i	θ_i
1	0	0	h	0
2	0	0	0	$\theta + 90^\circ$
3	90°	0	r	0

$$\left[\begin{matrix} B \\ F \\ T \end{matrix} \right] = \begin{bmatrix} -s\theta & 0 & c\theta & rc\theta \\ c\theta & 0 & s\theta & rs\theta \\ 0 & 1 & 0 & h \\ 0 & 0 & 0 & 1 \end{bmatrix}$$

$$h = P_Z \quad \theta = \tan^{-1}\left(\frac{P_Y}{P_X}\right) \quad r = \sqrt{P_X^2 + P_Y^2}$$

There is one solution, assuming positive r .

Cylindrical II Regional Arm

Table A.4 Cylindrical II DH Parameters

i	α_{i-1}	a_{i-1}	d_i	θ_i
1	0	0	h	0
2	0	0	0	θ
3	0	r	0	0

Spherical Regional Arm

Table A.5 Spherical DH Parameters

i	α_{i-1}	a_{i-1}	d_i	θ_i
1	0	0	0	θ
2	90°	0	0	$\phi + 90^\circ$
3	90°	0	r	0

$$\left[\begin{matrix} B \\ F \\ T \end{matrix} \right] = \begin{bmatrix} -s\theta & -c\theta s\phi & c\theta c\phi & rc\theta c\phi \\ c\theta & -s\theta s\phi & s\theta c\phi & rs\theta c\phi \\ 0 & c\phi & s\phi & rs\phi \\ 0 & 0 & 0 & 1 \end{bmatrix}$$

$$\theta = \tan^{-1}\left(\frac{P_Y}{P_X}\right) \quad \phi = \tan^{-1}\left(\frac{P_Z c\theta}{P_X}\right) \quad r = \sqrt{P_X^2 + P_Y^2 + P_Z^2}$$

There are two solutions.

Articulated Regional Arm

Table A.6 Articulated DH Parameters

i	α_{i-1}	a_{i-1}	d_i	θ_i
1	0	0	0	θ_1
2	90°	L_1	0	θ_2
3	0	L_2	0	$\theta_3 + 90^\circ$
4	90°	0	L_3	$\theta_4 + 90^\circ$

$$\begin{bmatrix} B \\ F \\ T \end{bmatrix} = \begin{bmatrix} s_1 & c_1 s_{23} & c_1 c_{23} & L_1 c_1 + L_2 c_1 c_2 + L_3 c_1 c_{23} \\ -c_1 & s_1 s_{23} & s_1 c_{23} & L_1 s_1 + L_2 s_1 c_2 + L_3 s_1 c_{23} \\ 0 & -c_{23} & s_{23} & L_2 s_2 + L_3 s_{23} \\ 0 & 0 & 0 & 1 \end{bmatrix}$$

$$\theta_2 + \theta_3 = 2 \tan^{-1} \left(\frac{-2L_3 P_Z \pm \sqrt{4L_3^2 (K_3^2 + P_Z^2) - (L_2^2 - L_3^2 - K_3^2 - P_Z^2)^2}}{L_2^2 - L_3^2 - K_3^2 - P_Z^2 - 2L_3 K_3} \right)$$

$$\theta_1 = \tan^{-1} \left(\frac{P_Y}{P_X} \right) \quad \theta_2 = \tan^{-1} \left(\frac{P_Z - L_3 s_{23}}{K_3 - L_3 c_{23}} \right) \quad \theta_3 = (\theta_2 + \theta_3) - \theta_2$$

where: $K_3 = P_X c_1 + P_Y s_1 - L_1$

There are four solutions.

For the Cartesian, cylindrical, and spherical regional arms, the DH parameters of the overall manipulator are obtained by adding Rows 4-*H* of Table A.1 to Rows 1-3 of the appropriate regional arm table. However, for the articulated regional arm, Row 4 is given in Table A.6, and the remaining rows are 5-*H* from Table A.1.